

# Design, Synthesis, and Biological Evaluation of a Series of Fluoroquinoanthrozazines with Contrasting Dual Mechanisms of Action against Topoisomerase II and G-Quadruplexes

Mu-Yong Kim,<sup>†,‡</sup> Wenhui Duan,<sup>†,‡</sup> Mary Gleason-Guzman,<sup>†</sup> and Laurence H. Hurley<sup>†,§,||,\*</sup>

College of Pharmacy, The University of Arizona, 1703 E. Mabel, Tucson, Arizona 85721, Division of Medicinal Chemistry, College of Pharmacy, The University of Texas at Austin, Austin, Texas 78712, Arizona Cancer Center, 1515 N. Campbell Avenue, Tucson, Arizona 85724, and Department of Chemistry, The University of Arizona, Tucson, Arizona 85721

Received August 6, 2002

Topoisomerase inhibitors are important and clinically effective drugs, while G-quadruplex-interactive compounds that disrupt telomere maintenance mechanisms have yet to be proven useful in the clinic. If G-quadruplex-interactive compounds are to be clinically useful, it will most likely be in combination with more established cytotoxic agents. We have previously reported on a family of topoisomerase II inhibitors that also interact with G-quadruplexes. On the basis of previously established structure–activity relationships (SARs) for compounds that are able to inhibit topoisomerase II or interact with G-quadruplex to varying degrees, we have now designed and synthesized four new fluoroquinoanthrozazines (FQAs) that have different profiles of mixed topoisomerase II poisoning effects and G-quadruplex interactions. The biological profiles of the four new compounds were determined with respect to G-quadruplex interaction (polymerase stop and photocleavage assays) and topoisomerase II interaction (DNA cleavage and kDNA decatenation assays), alongside cytotoxicity tests with matched pairs of topoisomerase II-resistant and topoisomerase II-sensitive cells and with telomerase (+) and ALT (+) cell lines (ALT = alternative lengthening of telomeres). From this study, we have identified two FQAs with sharply contrasting profiles of potent G-quadruplex interaction with a weak topoisomerase II poisoning effect, and vice versa, for further evaluation to determine the optimum combination of these activities in subsequent *in vivo* studies.

## Introduction

The fluoroquinolones (e.g., norfloxacin; see Figure 1 for structures) are well-known antimicrobial agents that inhibit bacterial DNA gyrase,<sup>1,2</sup> but more recently some tetracyclic quinolone analogues have shown good anti-neoplastic activity, which is most probably mediated by interaction with eukaryotic type II topoisomerase (topoisomerase II). Topoisomerase II is an enzyme that catalyzes changes in the topology of DNA via a mechanism involving the transient double-strand breaking and rejoining of phosphodiester bonds in DNA.<sup>3,4</sup> This enzyme plays several key roles in the DNA metabolism and chromosome structure, and it is the primary cytotoxic target for a number of potent anticancer drugs, including the anthracyclines, acridines, and epipodophyllotoxins.<sup>5,6</sup> On the basis of their mechanism of action, the topoisomerase II inhibitors are classified into two groups: (1) topoisomerase II poisons, which interfere with the breaking-rejoining reaction of the enzyme by trapping the covalent reaction intermediates, known as the cleaved complexes, and (2) catalytic inhibitors that inhibit the activity of topoisomerase II at a step prior to the formation of the cleaved complex.<sup>7</sup>

The quinobenzoxazine A-62176 (1-(3-aminopyrrolidin-1-yl)-2-fluoro-4-oxo-4*H*-quino[2,3,4-*ij*][1,4]benzoxazine-5-carboxylic acid; Figure 1) is a fluoroquinolone analogue that shows good activity against a number of human and murine cancer cell lines, including the multidrug-resistant P388/ADR line *in vitro* and several murine and human tumors *in vivo*.<sup>8–10</sup> Permana and co-workers have shown that A-62176 belongs to the class of catalytic inhibitors of topoisomerase II.<sup>11</sup> Our experimental results are in accord with the Permana study, but we also demonstrate that A-62176 acts as a topoisomerase II poison under certain conditions with specific DNA sequences.<sup>12</sup> The planar tetracyclic ring structure of A-62176, in contrast to the bicyclic ring system of a typical antibacterial fluoroquinolone, enables it to interact with duplex DNA and the more expansive planarity of G-quadruplex structures.<sup>13</sup> G-quadruplex structures are known to inhibit telomerase activity by sequestration of the substrate required for enzyme activity,<sup>14</sup> and therefore small organic molecules that stabilize or induce G-quadruplex structures have been suggested as potential anticancer therapeutic agents.<sup>15</sup> (For a recent review, see Neidle and Parkinson, 2002.<sup>16</sup>) Indeed, a number of G-quadruplex-interactive compounds have been demonstrated to not only inhibit telomerase activity in cell-free and *in vitro* systems but also to cause effects such as telomere shortening, anaphase bridge formation, and cell crisis in cancer cells.<sup>13,17–20</sup>

\* To whom correspondence should be addressed. Tel: 520 626-5622. Fax: 520 626-5623. E-mail: hurley@pharmacy.arizona.edu.

<sup>†</sup> College of Pharmacy, The University of Arizona.

<sup>‡</sup> Division of Medicinal Chemistry, College of Pharmacy, The University of Texas at Austin.

<sup>§</sup> Arizona Cancer Center.

<sup>||</sup> Department of Chemistry, The University of Arizona.

<sup>‡</sup> Present address: Shanghai Institute of Materia Medica, Chinese Academy of Sciences, Shanghai, 200031.

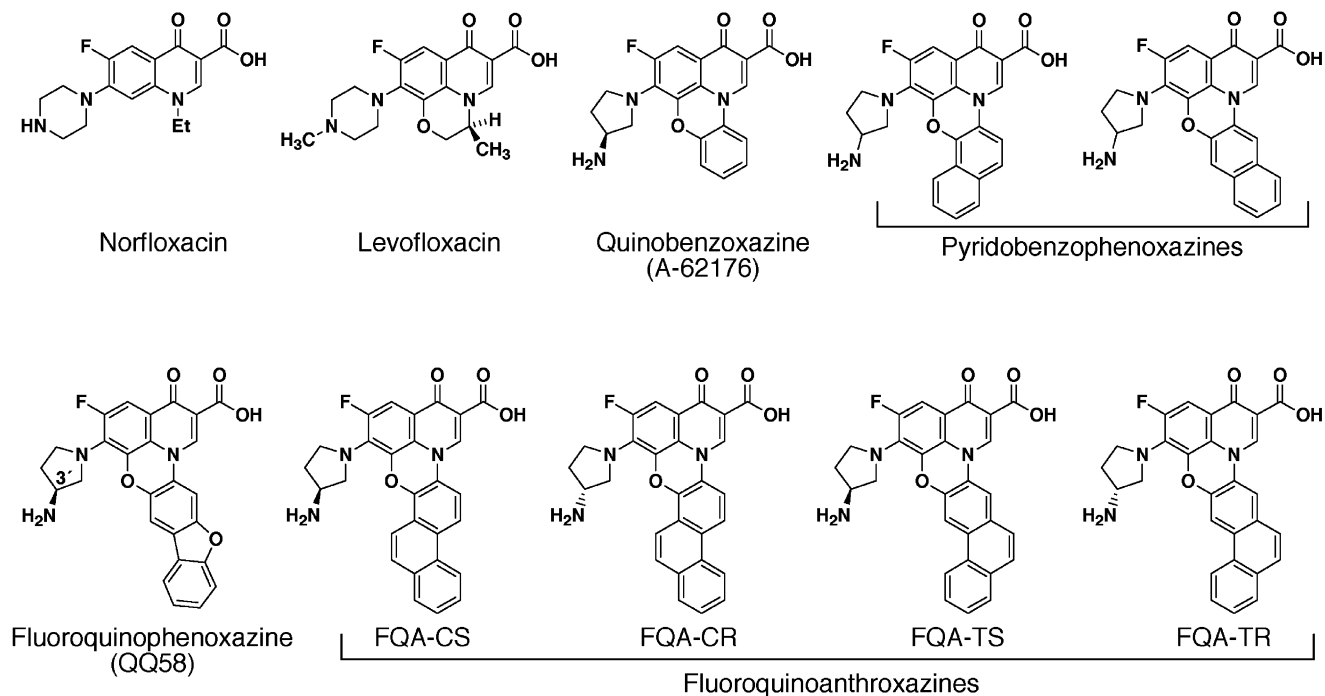


**Figure 1.** Chemical structures of fluoroquinolone analogues and FQAs.

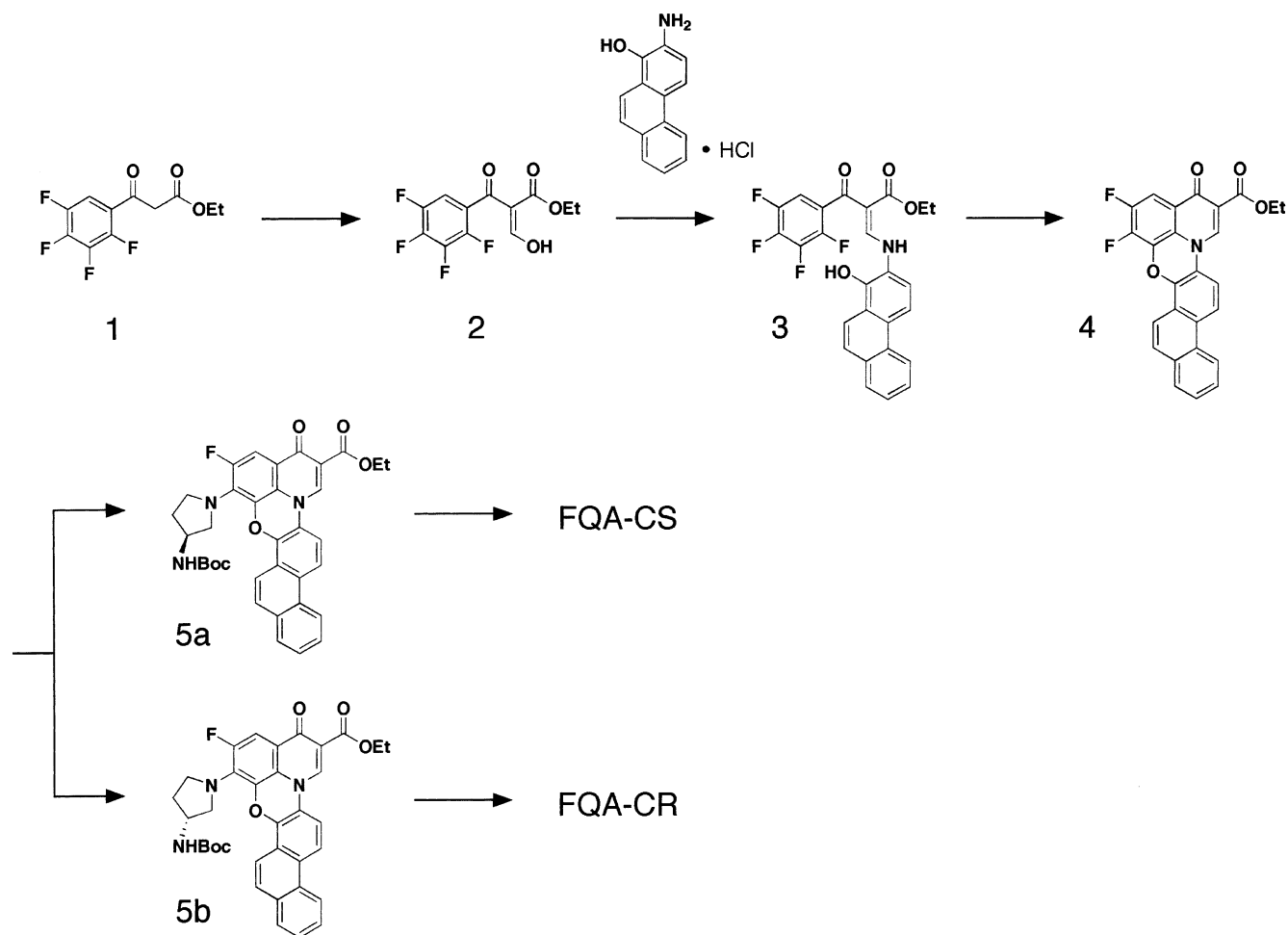
Previously, A-62176 has served as the starting point for the design of QQ58, a fluoroquinophenoxazine (Figure 1).<sup>13</sup> The extended phenoxazine ring of QQ58 selectively enhances its stacking interactions with G-quadruplex structures, thereby increasing telomerase inhibition. Moreover, QQ58 loses the topoisomerase II poisoning effects of its parent drug. Topoisomerase II poisons typically show better clinical activity than catalytic inhibitors, most probably because of their DNA damage and apoptosis signaling. To increase the G-quadruplex interactions while still maintaining the topoisomerase II poisoning effects, we have now designed and synthesized a series of FQAs on the basis of previously established SARs for compounds that possess varying degrees of topoisomerase II or G-quadruplex interactions.<sup>13,21</sup> The overall objective was to identify two or more compounds with contrasting topoisomerase II poisoning abilities and G-quadruplex interactions such that one compound would possess primarily topoisomerase II poisoning abilities and the other primarily the ability to interact with G-quadruplex. We have analyzed this series of FQAs for G-quadruplex and topoisomerase II inhibitions using polymerase stop assays, photocleavage studies, DNA cleavage assays, and kDNA decatenation assays. Biological assays, i.e., assays that measure cytotoxicities in topoisomerase II-resistant and topoisomerase II-sensitive cells and activities in telomerase (+) and ALT (+) cell lines, have also been conducted to establish the basis for the biological activity of the FQAs. We have successfully identified two FQAs that have appropriate contrasting activities as topoisomerase II poisons and G-quadruplex-interactive compounds for further studies.

## Results

**Design of the Fluoroquinoanthroxazines.** As stated previously, A-62176 served as the starting point for the design of QQ58 (Figure 1). In contrast to the various modes of action of A-62176, which include its

targeting of topoisomerase II and the topoisomerase II–DNA complex and its modest G-quadruplex interactions, QQ58 was found to exhibit enhanced stacking interactions with G-quadruplex structures and thereby shows increased telomerase inhibition and associated biological effects.<sup>13</sup> However, QQ58 did not retain the topoisomerase II poisoning activity of the parent drug (A-62176) because of the loss of interaction with the topoisomerase II–DNA complex. In the current study we have extended the aromatic ring system of A-62176 by introducing a naphthyl group, with the aim of increasing the stacking interactions with G-quadruplex structures or increasing the interactions with topoisomerase II–DNA complexes. It was envisaged that this naphthyl group would confer a similar increase in activity against human topoisomerase II, as was previously observed when a single phenyl ring extension was introduced in the pyridobenzophenoxazines (structures shown in Figure 1) in the appropriate orientation.<sup>21</sup> The configuration at the 3'-C aminopyrrolidine carbon of QQ58 determines the disposition of the primary amino group in that ring and, consequently, its mode of interaction with the sugar phosphate DNA backbone of the G-quadruplex structure.<sup>13</sup> With these insights, the FQAs with two orientations for phenyl extensions were selected (Figure 1). (For ease of reference these are classified as either cis (C) or trans (T), depending on the orientation of the phenyl extension with respect to the remainder of the structure.) Also, the chirality at the 3'-C aminopyrrolidine carbon in these compounds gives rise to two enantiomers, *S* and *R*, for each cis and trans fluoroquinolone, and therefore four novel stereoisomeric FQAs were prepared: FQA-CS, FQA-CR, FQA-TS, and FQA-TR.

**Synthesis of the Fluoroquinoanthroxazines.** The synthetic procedure (Scheme 1) was based on a published method for the synthesis of the quinobenzoxazines, with some modification.<sup>8</sup> The synthesis was started with ethyl 2,3,4,5-tetrafluorobenzoyl acetate (**1**),

**Scheme 1.** Chemical Synthesis of FQA-CS and FQA-CR

which was prepared according to published procedure.<sup>8,13,21</sup> Treatment of 2,3,4,5-tetrafluorobenzoyl acetate with triethyl orthoformate in acetic anhydride followed by 2-amino-1-hydroxyphenanthrene hydrochloride generated the enamino keto acid intermediate **3**. The intermediate was treated with sodium hydrogen carbonate to complete the double annulation to give compound **4**. Regioselective nucleophilic substitution of the fluoride in compound **4** with 3-(*R*)- or (*S*)-(tert-butoxycarbonylamino)pyrrolidine gave the key intermediates **5a** and **5b**. Target molecules FQA-CS and FQA-CR were prepared by hydrolysis and deprotection of compounds **5a** and **5b**. FQA-TS and FQA-TR were synthesized using the same procedure, substituting 2-amino-3-hydroxyphenanthrene hydrochloride for 2-amino-1-hydroxyphenanthrene hydrochloride.

**Characterization of G-Quadruplex Interactions of the Fluoroquinoanthroxazines. The FQA-CR Isomer Is the Most G-Quadruplex-Stabilizing Compound in the FQA Series.** To determine the binding affinity of the FQAs with the intramolecular G-quadruplex structures, a DNA template containing four repeats of the human telomeric sequence TTAGGG was incubated with increasing concentrations of FQAs in the presence of *Taq* DNA polymerase.<sup>22</sup> The principle of the assay is shown to the left of the gel in Figure 2. DNA pausing occurs at the G-quadruplex forming site, the extent of which can be used as a measure of the interaction of the FQAs with G-quadruplex structures.<sup>23</sup>

However, for the human telomeric sequence, the high concentration of monovalent cations required to stabilize the G-quadruplex structure (60 mM NaCl and 60 mM KCl) caused nonspecific stops, even in the absence of FQAs (Figure 2). But even in this system it was apparent that FQA-CR showed a modest but selective stabilization of the G-quadruplex structure. To increase the sensitivity of this assay, the *Tetrahymena* telomeric sequence, which has four consecutive guanines in each telomeric sequence (TTGGGG), was employed in further studies, allowing the use of more modest concentrations of salts (5 mM KCl and 5 mM NaCl).<sup>22</sup> In the absence of compounds there is only a slight *Taq* polymerization pause at the G-quadruplex-forming site, while significantly greater pausing is observed at the same position in the presence of the higher concentrations of compounds (Figure 3, A and B). The IC<sub>50</sub> values of FQA-CS, FQA-CR, FQA-TS, and FQA-TR for the inhibition of enzyme processing were found to be 0.67, 0.06, 5.7, and 2.4 μM, respectively. The pausing of polymerase processing at the primer position in the presence of FQA-CR at a concentration of 10 μM is most likely due to the affinity of FQA-CR for single- and/or double-stranded DNA. These results demonstrate that FQA-CR has a selectivity of about 90-fold for G-quadruplex structures over single- and/or double-stranded DNA (Figure 3C).

To investigate the role of chromophore extension on G-quadruplex interaction, the polymerase stop reaction

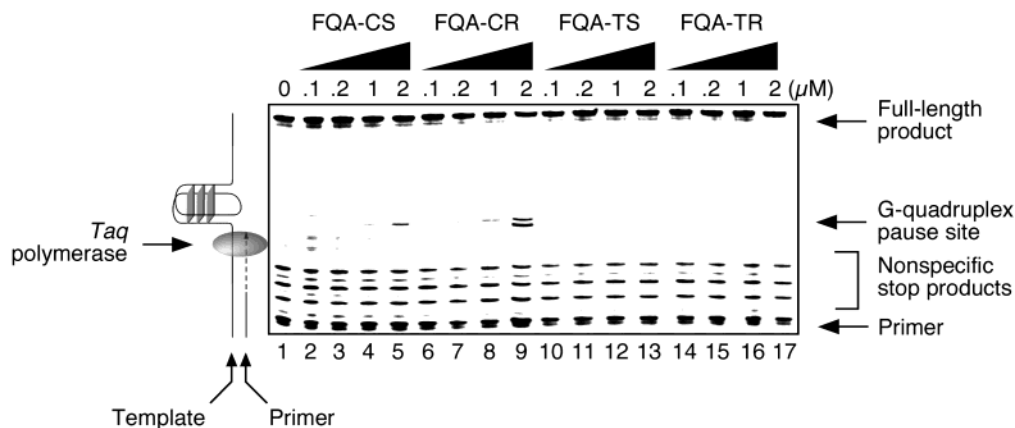


**Figure 2.** Concentration-dependent inhibition of polymerase DNA synthesis by the G-quadruplex structure formed on the DNA template containing the human telomeric sequence. Autoradiogram of a sequencing gel showing enhanced polymerase pausing at the G-quadruplex site with increasing concentrations of FQAs. Oligomer HT4 was incubated in reaction buffer (50 mM Tris-HCl, pH 7.5, 60 mM NaCl, 60 mM KCl, 10 mM MgCl<sub>2</sub>, 0.5 mM DTT, 0.1 mM EDTA, and 1.5 μg/μL BSA) in the presence of *Taq* DNA polymerase. Arrows indicate the positions of the full-length product of DNA synthesis, the G-quadruplex pause site, nonspecific stop products, and the free primer. End-labeled DNA was incubated under the same conditions without compound (lane 1). Lanes 2–5, 6–9, 10–13, and 14–17 contain increasing concentrations of FQA-CS, FQA-CR, FQA-TS, and FQA-TR, respectively. The cartoon on the left illustrates the principles of the assay.

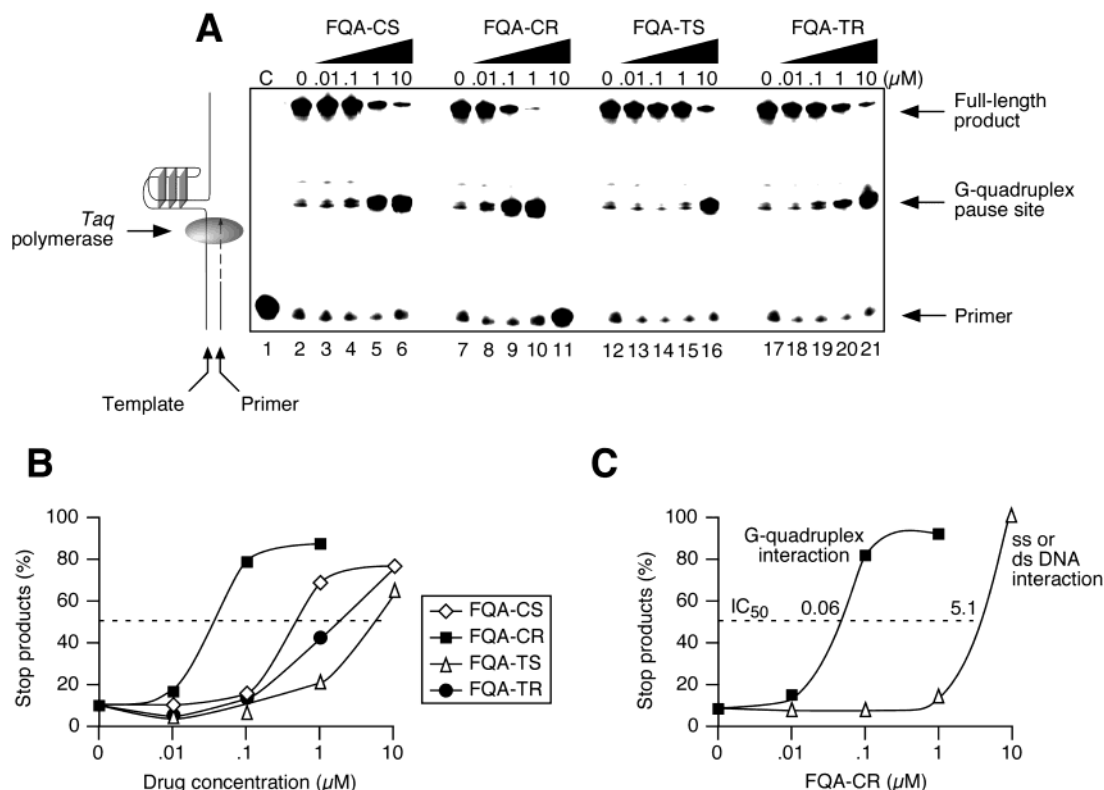


**Figure 3.** Concentration-dependent inhibition of polymerase DNA synthesis by the G-quadruplex structure formed on the DNA template containing the *Tetrahymena* telomeric sequence. (A) Autoradiogram of a sequencing gel showing enhanced polymerase pausing at the G-quadruplex site with increasing concentrations of FQAs. Oligomer PQ74 was incubated in reaction buffer (50 mM Tris-HCl, pH 7.5, 5 mM NaCl, 5 mM KCl, 10 mM MgCl<sub>2</sub>, 0.5 mM DTT, 0.1 mM EDTA, and 1.5 μg/μL BSA) in the presence of *Taq* DNA polymerase. Arrows indicate the positions of the full-length product of DNA synthesis, the G-quadruplex pause site, and the free primer. End-labeled DNA was incubated under the same conditions without compound (lane 1). Lanes 2–6, 7–11, 12–16, and 17–21 contain increasing concentrations of FQA-CS, FQA-CR, FQA-TS, and FQA-TR, respectively. The cartoon on the left illustrates the principles of the assay. (B) Graphical representation of the quantification of the sequencing gel shown in A, showing the percentage of stop product at the G-quadruplex site as a percentage of the total intensity per lane. (C) Graphical representation of the quantification of the stop products caused by the interaction of G-quadruplex or double-stranded DNA with FQA-CR.

was carried out with several quinolone analogues that have incrementally extended aromatic ring systems. As shown in Figure 4, compounds with more extended chromophores have higher G-quadruplex interactions.

In the TRAP assay, FQA-CR and FQA-CS had IC<sub>50</sub> values of 5.6 and 21 μM, respectively.

**The (TTGGGG)<sub>4</sub> Sequence Forms a Chair-Type G-Quadruplex in Which FQA-CR Interacts by**



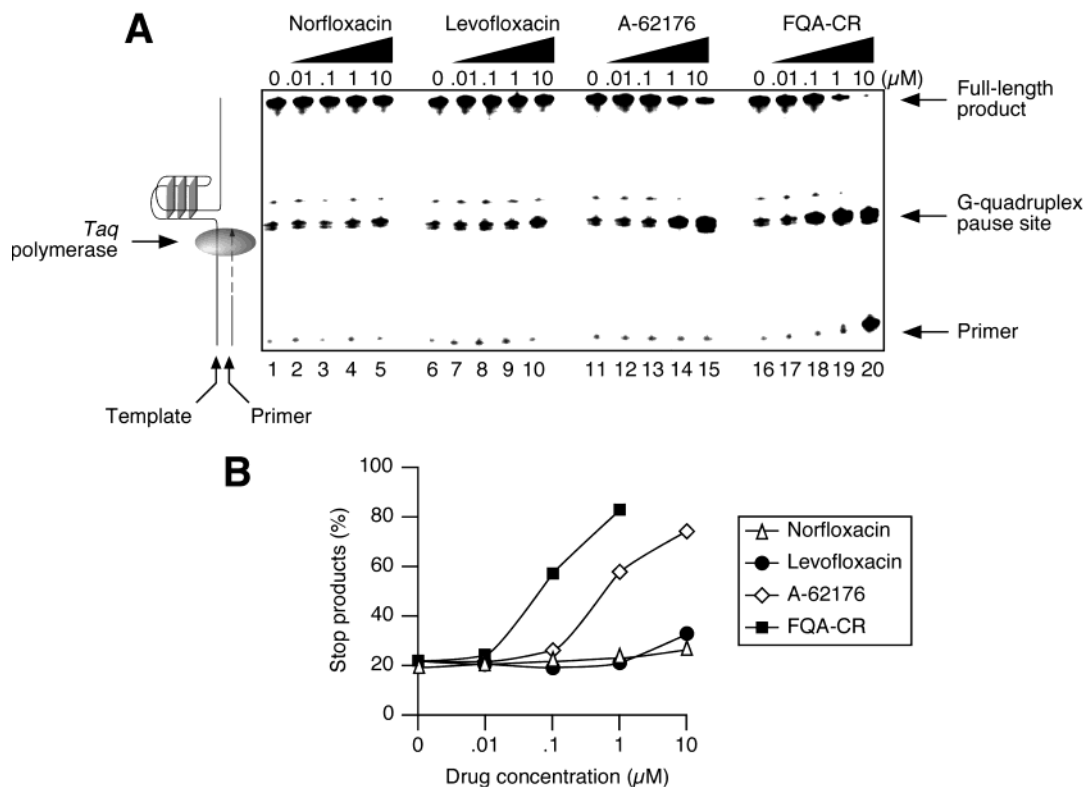


**Figure 4.** The effect of extending the chromophore on inhibition of the polymerase DNA synthesis at the G-quadruplex structure. (A) Autoradiogram of a sequencing gel showing enhanced polymerase pausing at the G-quadruplex site with increasing concentrations of FQAs. Oligomer PQ74 was incubated in reaction buffer (50 mM Tris-HCl, pH 7.5, 5 mM NaCl, 5 mM KCl, 10 mM MgCl<sub>2</sub>, 0.5 mM DTT, 0.1 mM EDTA, and 1.5  $\mu\text{g}/\mu\text{L}$  BSA) in the presence of *Taq* DNA polymerase. (B) Graphical representation of the quantification of the sequencing gel in A, showing the percentage of stop product at the G-quadruplex site as a percentage of the total intensity per lane.

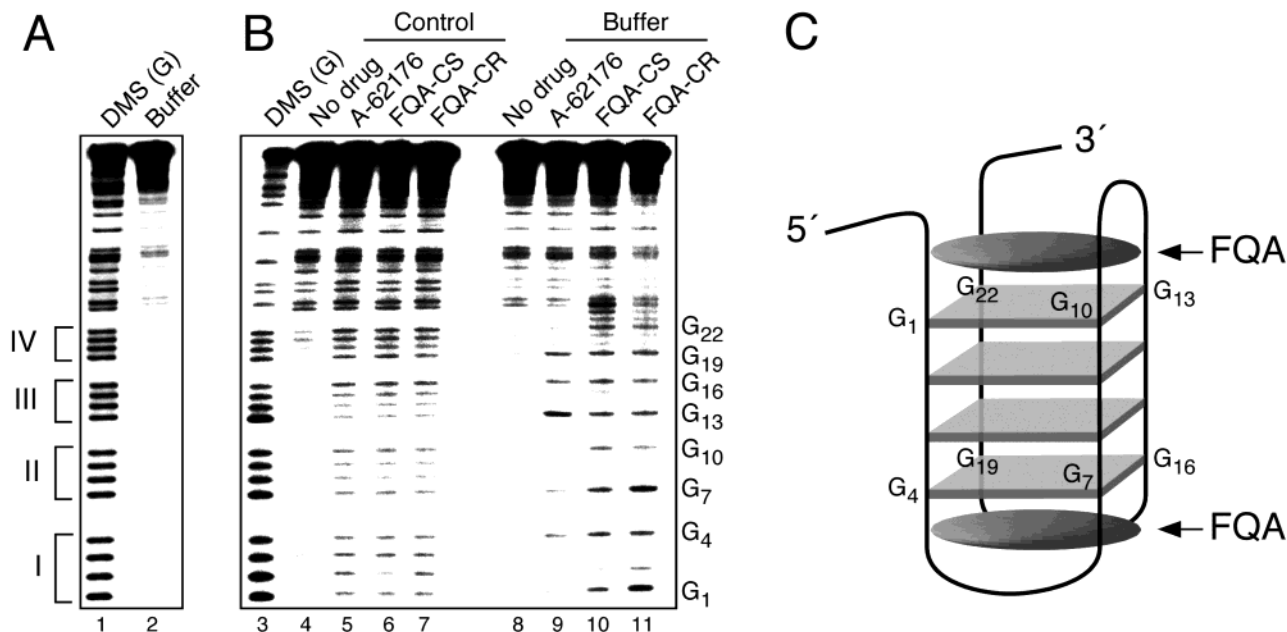


**Figure 5.** DMS methylation and photocleavage pattern of the PQ74 template in the presence of A-62176, FQA-CS, and FQA-CR. (A) DMS methylation protection of the PQ74 in Tris buffer (lane 1) or in reaction buffer containing 50 mM Tris-HCl, pH 7.5, 5 mM NaCl, 5 mM KCl, 10 mM MgCl<sub>2</sub>, 0.5 mM DTT, 0.1 mM EDTA, and 1.5  $\mu\text{g}/\mu\text{L}$  BSA (lane 2). Brackets I–IV indicate the four telomere G-quadruplex repeat sequences. (B) Photocleavage pattern of the PQ74 in Tris buffer (lanes 4–7) or in reaction buffer (lanes 8–11) in the presence of fluoroquinolones. Lane 3 shows DMS cleavage of denatured DNA. (C) Proposed model of FQAs binding to the intramolecular chair-type G-quadruplex structure. The numbers G1, G4, G7, G10, G13, G16, G19, and G21 correspond to the cleavage sites in (B), right panel. The FQA molecules are indicated by arrows.

**External Stacking within the Loop Regions.** A methylation protection assay was conducted to determine the likely G-quadruplex structure that produces

the stop in processivity of *Taq* DNA polymerase.<sup>24</sup> As shown in lane 1 of Figure 5, no apparent protection of any guanine was detected in the control in which the

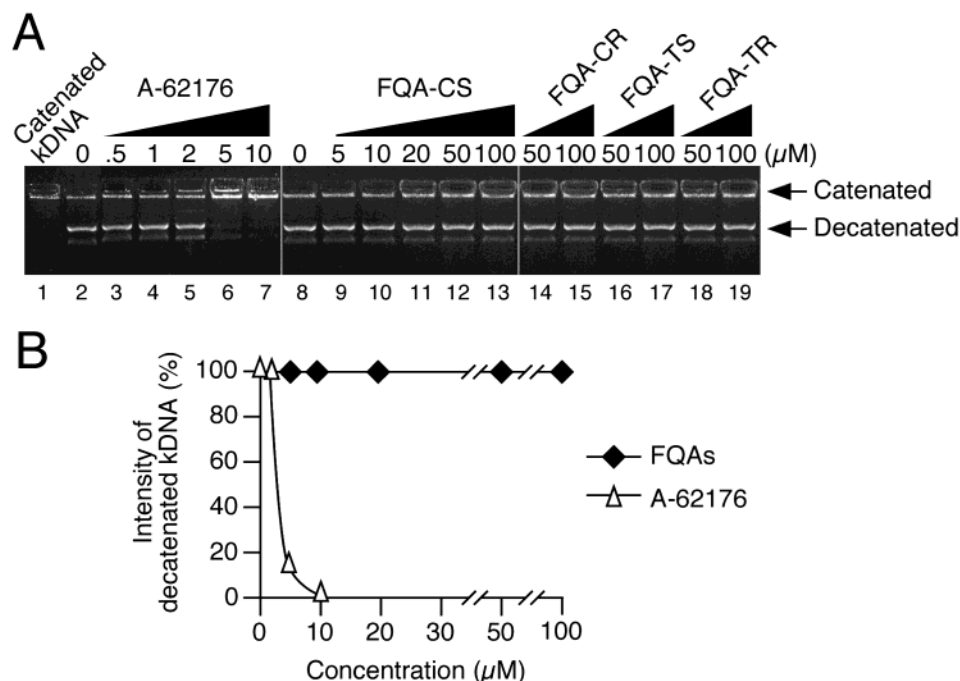


**Figure 6.** Inhibition of kDNA decatenation of human topoisomerase II by fluoroquinolones. (A) Catenated kDNA (0.25  $\mu\text{g}$ ) was treated with 2 units of human topoisomerase II in the presence of A-62176 or FQAs and then analyzed on 1% agarose gel. Arrows indicate the positions of the catenated and decatenated forms of kDNA. Lane 1 contains catenated kDNA only. Lanes 2 and 8 contain only kDNA and topoisomerase II. Lanes 3–7 contain 0.5, 1, 2, 5, and 10  $\mu\text{M}$  of A-62176, respectively. Lanes 9–13 contain 5, 10, 20, 50, and 100  $\mu\text{M}$  of FQA-CS, respectively. Lanes 14 and 15 contain 50 and 100  $\mu\text{M}$  of FQA-CR. Lanes 16 and 17 contain 50 and 100  $\mu\text{M}$  of FQA-TS. Lanes 18 and 19 contain 50 and 100  $\mu\text{M}$  of FQA-TR. (B) Intensity of decatenated kDNA was quantitated from the gel using ImageQuant software.

PQ74 template was incubated with dimethyl sulfate (DMS) in Tris buffer. However, all guanines in the G-quadruplex-forming site were protected from methylation in the buffer conditions of the polymerase stop assay. This DMS protection pattern is consistent with G-quadruplex structures in which all guanines participate in G-tetrad formation. The incubation conditions of 20 min with 10 nM of template DNA used in the polymerase stop and methylation protection assays favor the formation of intramolecular G-quadruplex structures,<sup>22</sup> in contrast to the formation of intermolecular G-quadruplex structures, which usually require incubation at micromolar concentrations of DNA for several hours.<sup>25</sup> To characterize the binding mode of the FQAs to this intramolecular G-quadruplex structure, a photomediated cleavage reaction was carried out. The photoreactive properties of the FQAs lead to strand cleavage around their binding site(s) that can then be used to determine the location of the FQAs in the G-quadruplex–drug complex.<sup>13</sup> In contrast to the low level of uniform photocleavage for all guanines of the PQ74 in Tris buffer (lanes 5–7 in Figure 5B), there is selective cleavage at the guanines located in tetrads at both ends of the G-quadruplex (G1, G10, G13, G22, and G4, G7, G16, and G19) in the presence of the buffer used in the polymerase stop assay (Figure 5B, lanes 9–11). On the basis of the DMS protection and photocleavage results, a model is proposed in which two FQA molecules selectively bind to the intramolecular chair-type G-quadruplex structure through an end-stacking binding mode (Figure 5C).

**Characterization of Topoisomerase II Inhibition. FQA Analogues Have Lost the Topoisomerase II Catalytic Activity of A-62176.** The effects of the

FQAs on the activity of human topoisomerase II were measured by means of a kDNA decatenation assay, which is routinely used to screen the inhibitors that specifically block the catalytic activity of topoisomerase II.<sup>26</sup> The parent compound, A-62176, was found to inhibit 50% of decatenation activity of topoisomerase II at a concentration of 3.2  $\mu\text{M}$ , while no inhibition was observed for the FQAs, even at a concentration of 100  $\mu\text{M}$  (Figure 6). This result shows that the FQAs have no effect on the catalytic activity of topoisomerase II.

**Whereas A-62176 Is Both a Topoisomerase II Poison and a Catalytic Inhibitor, the FQAs Are Only Topoisomerase II Poisons.** During the breaking and rejoining process, topoisomerase II forms a covalent bond with the cleaved DNA to maintain the integrity of DNA.<sup>2</sup> Topoisomerase II poisons increase the amount of DNA breakage by enhancing the steady-state levels of the covalent reaction intermediates, termed the topoisomerase II–DNA complexes, which are normally short-lived under physiological conditions.<sup>4,5</sup> In contrast, catalytic inhibitors decrease the level of double-strand breakage because they inhibit the formation of the aforementioned complexes. Additional characterization of the effects of the FQAs on the activity of topoisomerase II was determined by a DNA cleavage assay. At higher concentrations of all four FQAs, the intensity of topoisomerase II-mediated DNA cleavage was significantly increased (lanes 8 and 9, 13 and 14, 19 and 20, and 24 and 25 in Figure 7A). The degree of poisoning activity of the FQAs was in the decreasing order FQA-CS > FQA-CR > FQA-TS > FQA-TR, with FQA-CS being by far the most potent (Figure 7B). The extent of topoisomerase II poisoning activity of FQA-CS was compared with that of A-62176 (Figure 7C). The inten-

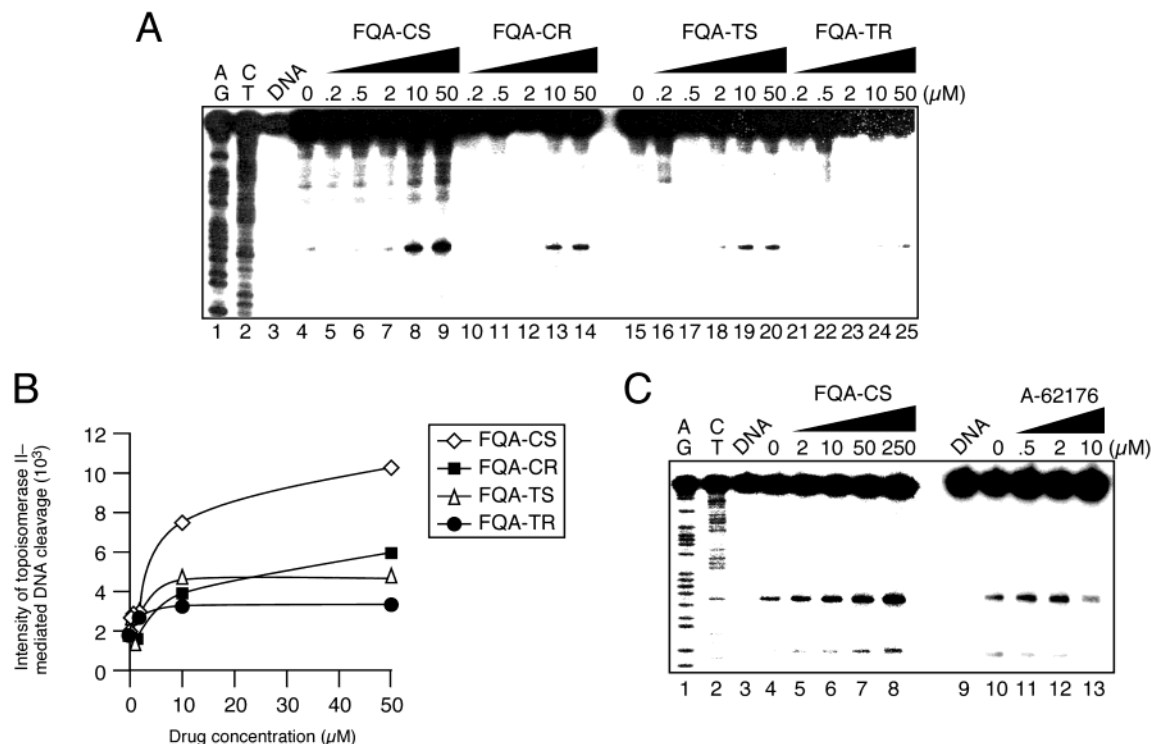


**Figure 7.** Effects of FQAs and A-62176 on DNA cleavage activity of human topoisomerase II. (A) Autoradiogram of a denaturing polyacrylamide gel showing the topoisomerase II-mediated DNA cleavage pattern in the presence of FQAs. Lanes 4 and 15 contain only DNA and topoisomerase II. Lanes 5–9, 10–14, 16–20, and 21–25 contain 0.2, 0.5, 2, 10, and 50  $\mu\text{M}$  of FQA-CS, FQA-CR, FQA-TS, and FQA-TR, respectively. (B) Graphical representation of the quantification of the sequencing gel in A, showing the percentage of stop product at the G-quadruplex site as a percentage of the total intensity per lane. (C) Autoradiogram of a denaturing polyacrylamide gel showing the topoisomerase II-mediated DNA cleavage pattern in the presence of FQA-CS or A-62176. The cleavage reaction was performed in the reaction buffer as described in the Experimental Section. Lanes 4 and 10 contain only DNA and topoisomerase II. Lanes 5–8 contain 2, 10, 50, and 250  $\mu\text{M}$  of FQA-CS. Lanes 11–13 contain 0.5, 2, and 10  $\mu\text{M}$  of A-62176.

sity of DNA cleavage increased in a concentration-dependent manner for FQA-CS, whereas for A-62176 the levels of DNA cleavage initially were increased at low concentrations but decreased at higher concentrations of this compound, presumably due to the topoisomerase II inhibitor effect of A-62176.<sup>12</sup> Taken together, the results of the kDNA decatenation and DNA cleavage assays demonstrate that the FQAs only retain the topoisomerase II poisoning activity of the parent compound, A-62176, in contrast to QQ58, which loses the topoisomerase II poisoning effect.

**In Vitro Activity. G-Quadruplex Interaction Is Critically Important in Determining the Cytotoxicity of the FQA Compounds.** In the previous sections we have shown that all four FQA compounds can act as topoisomerase II poisons and also interact with G-quadruplex structures. Importantly, the FQA compounds were found to possess different combinations of activity against these two targets. To compare the overall importance of topoisomerase II poisoning and G-quadruplex interaction, the cytotoxicities of the FQA compounds were tested against MCF7 breast cancer cells. The order of potency was FQA-CR > FQA-CS > FQA-TR > FQA-TS, and their  $\text{IC}_{50}$  values were 0.46, 1.1, 4.3, and 14.2  $\mu\text{M}$ , respectively (Figure 8). This order for cytotoxic potency corresponds best with the trend found for G-quadruplex interaction rather than that found for topoisomerase II poisoning. Therefore, this result suggests that G-quadruplex interaction is more

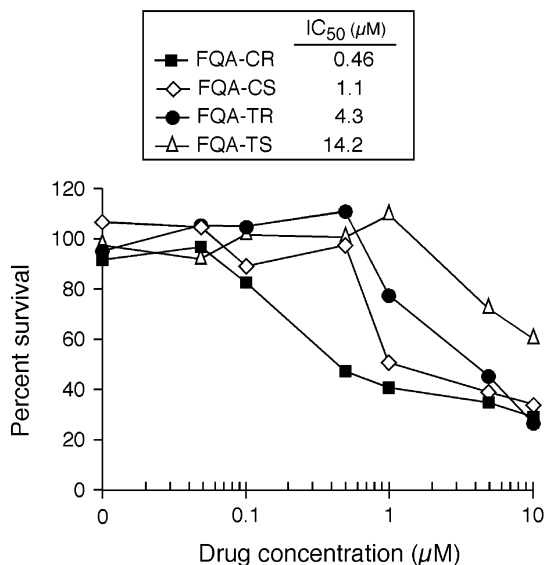


**Figure 8.** Effect of FQAs on the growth of MCF7 breast cancer cells. MCF7 cells were exposed to the indicated concentrations of FQA compounds. After 3 days, the cytotoxicity was assessed and expressed as a percentage of the survival of untreated cells (100%). Each experiment was performed four times at each point.

important than topoisomerase II poisoning in determining the cytotoxicity of new FQA compounds.

**Because of Its Potent Topoisomerase II Poisoning Effect, FQA-CS Shows Lower Activity against**

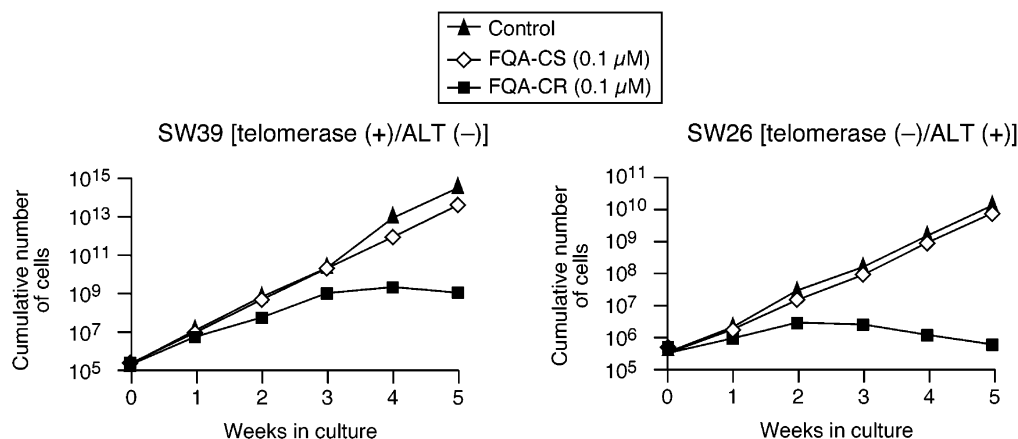


**Figure 9.** Effect of long-term exposure with nontoxic concentrations of FQA-CS and FQA-CR on the culture growth of SW39 [telomerase (+)/ALT (-)] and SW26 [telomerase (-)/ALT (+)]. SW39 and SW26 cells were exposed to a 0.1  $\mu\text{M}$  concentration of FQA-CS or FQA-CR. Pools of cells were passaged every 7 days by seeding  $\sim 10^5$  cells into a new 75-cm<sup>2</sup> flask. After counting the number of cells, the culture growth was plotted as a cumulative number of cells versus weeks in culture. Each experiment was performed four times at each point.

**Table 1.** Cytotoxicities of FQAs and Doxorubicin against 8226/S and 8226/DOX1V Cells<sup>a</sup>

drug	8226/S	8226/DOX1V	ratio (DOX1V/S)
doxorubicin	0.037 $\pm$ 0.001	0.320 $\pm$ 0.039	8.65
FQA-CS	0.690 $\pm$ 0.074	2.775 $\pm$ 0.242	4.02
FQA-CR	0.324 $\pm$ 0.013	0.501 $\pm$ 0.039	1.55
FQA-TS	>10	>10	ND
FQA-TR	5.46 $\pm$ 0.411	>10	ND

<sup>a</sup> 8226/S is a multiple myeloma cancer cell. 8226/DOX1V is a doxorubicin-resistant cell line of 8226/S. Average and standard deviation values were calculated from the four sets of experiments. (Average  $\pm$  standard deviation; unit:  $\mu\text{M}$ ).

**Topoisomerase II-Depleted Cells Than Topoisomerase II-Sensitive Cells, While FQA-CR Shows Equal Activity against Both Topoisomerase II-Sensitive and Topoisomerase II-Depleted Cells.** To further characterize the role of topoisomerase II interaction in determining the overall activity of the FQAs, the cytotoxicities of the FQAs against 8226/S (a human multiple myeloma cell line of RPMI 8226) and 8226/DOX1V (a doxorubicin-resistant cell line of 8226/S) were measured.<sup>27</sup> Decreased levels of topoisomerase II expression in 8226/DOX1V resulted in less drug-induced DNA cleavage and a corresponding decrease in cytotoxicity observed for doxorubicin (Table 1). FQA-CS, the strongest topoisomerase II poison among the compounds tested, showed a 4-fold decrease in activity against 8226/DOX1V cells relative to that seen against 8226/S cells. However, for FQA-CR, the most favored G-quadruplex-interactive compound, there was much less cytotoxicity difference between the two cell lines (1.55-fold). This implies that the overall cytotoxicity of FQA-CR in MCF7 cells is not due to topoisomerase II poisoning activity but is presumably due to its G-quadruplex interaction.

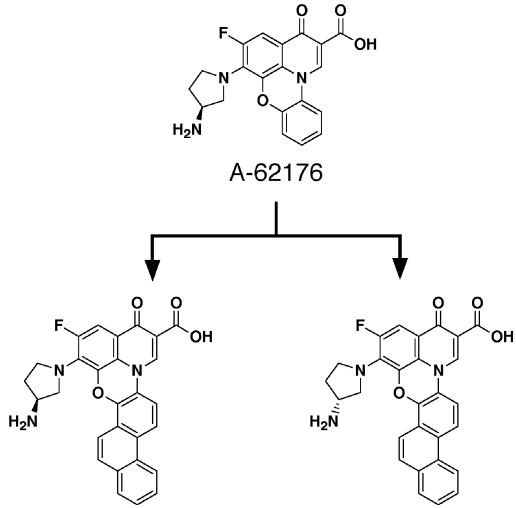
**FQA-CR Suppresses the Proliferation of Both Telomerase (+) and ALT (+) Cells at Noncytotoxic Concentrations, While FQA-CS Has Little Antiproliferative Effects.** The effects of FQA-CR and FQA-CS against SW39 [telomerase (+)/ALT (-)] and SW26 [telomerase (-)/ALT (+)]<sup>28</sup> were analyzed in order to evaluate the contribution of G-quadruplex interactions (Figure 9). Unlike telomerase inhibitors, G-quadruplex-interactive compounds are expected to suppress the proliferation of both telomerase (+) cells and ALT

(+) cells, which maintain their telomeres through the ALT mechanisms.<sup>29</sup> Long-term cytotoxic effects were compared for control cells and cells that had been treated for 5 weeks with noncytotoxic concentrations of FQA-CR and FQA-CS (0.1  $\mu\text{M}$ ). In both telomerase (+) and ALT (+) cells, we observed the suppression of cell proliferation within 1–2 weeks with FQA-CR, while cells treated with FQA-CS showed a similar growth curve to that of the control cells (Figure 9).

## Discussion

The objective of this study was the identification of new compounds with contrasting profiles of mixed topoisomerase II poisoning effects and G-quadruplex interactions. The initial lead compound was a quinobenzoxazine (A-62176), which is structurally related to the well-known class of fluoroquinolone antibiotics, e.g., norfloxacin. It was previously demonstrated that this quinobenzoxazine was a mammalian cytotoxic agent, shown to be both a topoisomerase II poison and catalytic inhibitor as well as a weak G-quadruplex-interactive compound. A-62176 then served as a template for the design of the fluoroquinophenoxazine compound QQ58, which has an expanded ring system and demonstrates enhanced stacking interactions with G-quadruplex structures but has lost the topoisomerase II poisoning activity of A-62176. The FQAs in this study were designed to combine the biological effects of G-quadruplex-interactive compounds with more established cytotoxic agents that act as topoisomerase II poisons. The polymerase stop and DNA cleavage assays provided important cell-free signatures of G-quadruplex interaction activity and topoisomerase II poisoning activity, respectively. Among the new FQAs synthesized, FQA-CS and FQA-CR fulfilled the required mix of the different types of activity (Table 2). The FQAs, containing an additional naphthyl ring in the cis orientation, are able to recognize and bind quite specifically to G-quadruplex structures and topoisomerase II–DNA complexes. Within the cis group, FQA-CR showed a higher G-quadruplex interaction, while FQA-CS showed more potent topoisomerase II poisoning activity. The results from this study are consistent with there being common molecular features of A-62176 and FQA molecules that appear critical for



**Table 2.** Summary of Biological Activities of FQA-CS and FQA-CR


	FQA-CS	FQA-CR
G-quadruplex interaction		
polymerase stop assay (IC <sub>50</sub> )	0.67 μM	0.06 μM
long-term effects <sup>a</sup>	no effect	senescence
topoisomerase II inhibition		
topoisomerase II poison effects	+++	+
cytotoxic ratio topoisomerase II-R/-S cells <sup>b</sup>	4.02	1.55
overall cytotoxicity		
MCF7 breast cells (IC <sub>50</sub> )	1.1 μM	0.46 μM
major mechanism of action	topoisomerase II poison	G-quadruplex interaction

<sup>a</sup> Effects of long-term exposure with nontoxic concentrations of FQA-CS and FQA-CR on the culture growth of SW39 [telomerase (+)/ALT (-)] and SW26 [telomerase (-)/ALT (+)]. <sup>b</sup> The ratio of cytotoxicity of FQA-CS and FQA-CR against 8226/DOX1V (topoisomerase II-resistant) and 8226/S (topoisomerase II-sensitive) cells.

the recognition of their receptors. These include the amphoteric nature of both molecules, the same intramolecular separation of the positive and negative charges, and the planar nature of both molecules. The extension of the naphthyl ring in the cis direction serves to increase the planar aromatic system while retaining the amphoteric nature of these compounds, and thus it enables the FQAs to interact strongly with G-quadruplex structures and topoisomerase II–DNA complexes. The parent compound, A-62176, has minimal stacking interactions, which results in insufficient  $\pi$ – $\pi$  stacking interactions to adequately stabilize G-quadruplex structures. The *R*-enantiomer of the FQAs containing a cis phenyl extension interacts with G-quadruplexes to a greater extent than does the *S*-enantiomer. This result is due to the amino hydrogen(s) of the aminopyrrolidine ring in the *R*-enantiomer being more favorably disposed than the corresponding *S*-enantiomer to facilitate the formation of a stabilizing hydrogen bonding interaction with the 5' phosphate group in the G-tetrad(s) of G-quadruplexes.<sup>13</sup> In contrast, the *S*-enantiomer is more favored for binding with topoisomerase II–DNA complexes.<sup>12,30</sup> Indeed, the results of the *Taq* polymerase assay (Figure 3A) show that FQA-CR is more selective for G-quadruplex structures than double-stranded DNA.

Telomeres are specialized functional DNA–protein complexes that protect the ends of eukaryotic chromosomes. The telomeric DNA is capped by a number of bound proteins, including TRF1 and TRF2.<sup>31–33</sup> Griffith and co-workers have demonstrated, using electron microscopy, that the human telomeric binding protein TRF1 can remodel telomeric DNA into a “T-loop,” which is a large duplex loop-back structure most likely formed

through the invasion of the single-stranded telomeric 3'-overhang into the duplex telomeric repeat.<sup>34</sup> Disruption of this T-loop by depletion of proteins involved in telomere binding (e.g., TRF2) leads to chromosomal end-to-end fusions in presenescence cells, implying that telomeric function is more likely to depend on structure, rather than on length alone.<sup>35</sup> G-quadruplex-interactive compounds also induce the end-to-end fusions of chromosomes in embryo cells, presumably by facilitating the formation of inappropriate telomeric end structures.<sup>13</sup> For example, the stabilization of dimeric G-quadruplex structures from two 3' telomeric overhangs may lead to end-to-end fusion of chromosomes. Among the four new FQA compounds, FQA-CR and FQA-CS were found to induce apparent end-to-end adherence of anaphase and telophase chromosomes in sea urchin embryos after relatively short periods of time (unpublished data). The abnormal chromosomes, including end-to-end fusions, would likely break during mitosis, resulting in severe damage to the genome and the activation of DNA damage checkpoints. This in turn should lead to cell senescence or the initiation of the apoptosis cell death pathway.<sup>35</sup> The induction of anaphase bridges could be a more important mechanism for FQA-CR and FQA-CS in killing cancer cells than the inhibition of telomerase activity.

FQA-CR suppressed the proliferation of both telomerase (+) and ALT (+) cells, an effect that occurs within one or two weeks at noncytotoxic concentrations. Unlike telomerase inhibitors, G-quadruplex-interactive compounds would be expected to affect cells that maintain telomeres by telomerase-dependent as well as telomerase-independent ALT mechanisms,<sup>18,29</sup>

since during the recombination process of the ALT mechanism, two chromosome ends need to be in close proximity. Therefore, G-quadruplex-interactive compounds can easily trap out or stabilize intermolecular G-quadruplexes and thereby cause the activation of DNA damage check points. G-quadruplex-interactive compounds, when bound to intermolecular G-quadruplexes, have been found to inhibit helicases such as Sgs1, which normally are able to clear G-quadruplex structures from DNA.<sup>36</sup>

Using crystallography, the Neidle laboratory recently has reported an alternative intramolecular G-quadruplex structure<sup>37</sup> for the human telomeric sequence to that reported by Patel.<sup>38</sup> In the case of the Patel NMR study, a basket-type structure was found using Na<sup>+</sup> ions. The Neidle structure is a propeller type, but the crystallization conditions were quite different, involving K<sup>+</sup> in place of Na<sup>+</sup>, and, significantly, in the presence of a G-quadruplex-interactive molecule, although the ligand did not appear in the final structure. All the experimental results reported here are consistent with targeting G-quadruplexes involving chair- or basket-type structures, although we certainly cannot rule out the involvement of the propeller type, even though there is little resemblance between the FQA compounds and the G-quadruplex ligand included in the Neidle crystallization study.

In conclusion, a novel group of FQAs has been designed and synthesized on the basis of previously established SARs for DNA-topoisomerase II and G-quadruplex interactions. Among them, FQA-CS and FQA-CR produce contrasting profiles of mixed topoisomerase II and G-quadruplex interactions and show potent inhibitory activity against tumor cell lines. These compounds are under further evaluation to determine the consequences of a dual mechanism of action against topoisomerase II and G-quadruplexes and to determine the optimum combination of these modes of action for activities *in vivo*.

In the cytotoxicity studies with topoisomerase II-sensitive and topoisomerase II-resistant cell lines, FQA-CS showed a significant decrease in activity in resistant cells. However, FQA-CR showed a similar level of potency against the topoisomerase II-resistant cells compared to topoisomerase II-sensitive cells. This might be an important advantage of drugs with a dual mechanism of action for treating tumors that already have resistance mechanisms for one specific target.

These results, taken together with the results from biological studies of G-quadruplex and topoisomerase II interactions, suggest that although both FQA-CS and FQA-CR show good *in vitro* activity against cancer cells, they have contrasting profiles of activity: FQA-CR has a potent G-quadruplex interaction with a weak topoisomerase II poisoning effect, and FQA-CS has a strong topoisomerase II poisoning effect with a weak G-quadruplex interaction. *In vivo* studies will be reported in due course.

## Experimental Section

**Chemistry.** All melting points were recorded on a Thomas-Hoover capillary melting point apparatus and are uncorrected. <sup>1</sup>H and <sup>13</sup>C NMR data were run on a Varian Unity 300-MHz NMR spectrometer. The chemical shifts are relative to the trace proton, carbon, or fluorine signals of the deuterated

solvent. Coupling constants, *J*, are reported in Hz and refer to apparent peak multiplicity and not true coupling constants. Elemental analysis of C, H, N was done by Quantitative Technologies Inc., White House, NJ. Flash column chromatography was performed on silica gel 60, 230–400 mesh, purchased from Spectrum. All starting materials were obtained from commercial sources unless otherwise specified.

**Ethyl 3-(1-Hydroxyphenanthren-2-ylamino)-2-(2,3,4,5-tetrafluorobenzoyl)acrylate (2).** A mixture of ethyl 2,3,4,5-tetrafluorobenzoyl acetate (220 mg, 0.83 mmol), acetic anhydride (350  $\mu$ L, 3.71 mmol), and triethyl orthoformate (210  $\mu$ L, 1.28 mmol) was stirred at 130 °C for 4 h. Excess acetic anhydride and triethyl orthoformate was removed *in vacuo*, and the residue was dried over a vacuum pump to give a pale yellow liquid, which was used in the next step without further purification. To this pale yellow liquid in methylene chloride (5 mL) was added a solution of 2-amino-1-hydroxyphenanthrene prepared by mixing 2-amino-1-hydroxyphenanthrene hydrochloride<sup>39</sup> (120 mg, 0.41 mmol) with pyridine (150  $\mu$ L, 1.84 mmol) in methylene chloride (5 mL). The resulting mixture was stirred at room temperature for 12 h. A yellow-green solid formed in the reaction and was collected by filtration and dried over a vacuum pump to give 150 mg (76.1%) of a product as a yellow-green powder: <sup>1</sup>H NMR (DMSO-*d*<sub>6</sub>):  $\delta$  8.87 (d, 1H, *J* = 7.9 Hz), 8.75 (m, 1H), 8.50 (m, 1H), 8.16 (m, 1H), 7.80 (m, 2H), 7.88 (d, 1H, *J* = 7.9 Hz), 7.67 (m, 4H) 4.03 (q, 2H, *J* = 6.9 Hz), 1.09 (t, 3H, *J* = 6.9 Hz). MS (CI) *m/z* 484 (MH<sup>+</sup>).

**Ethyl 1,2-Difluoro-4-oxo-4H-pyrido[3,2,1-kl]naphtho[2,1-f]phenoxazine-5-carboxylate (3).** A mixture of compound 2 (128 mg, 0.33 mmol), NaHCO<sub>3</sub> (140 mg, 1.67 mmol), and DMF (5 mL) was stirred at 100 °C for 2.5 h. TLC (methylene chloride:MeOH = 40:1) showed the reaction was complete, and the solvent was removed using a rotary evaporator. The residue was purified by flash column to give 110 mg (94%) of product as a gray powder: mp = 225–227 °C. <sup>1</sup>H NMR (DMSO-*d*<sub>6</sub>):  $\delta$  8.98 (s, 1H), 8.52 (d, 1H, *J* = 8.4 Hz), 8.43 (d, 1H, *J* = 8.4 Hz), 8.11 (d, 1H, *J* = 9.3 Hz), 7.87 (m, 1H), 7.83 (d, 1H, *J* = 9.3 Hz), 7.65 (m, 4H), 4.49 (q, 2H, *J* = 6.9 Hz), 1.50 (t, 3H, *J* = 6.9 Hz). MS (CI) *m/z* 444 (MH<sup>+</sup>).

**Ethyl (R)-1-(3-(tert-Butoxycarbonylamino)pyrrolidin-1-yl)-2-fluoro-4-oxo-4H-pyrido[3,2,1-kl]naphtho[2,1-f]phenoxazine-5-carboxylate (4).** A mixture of ethyl ester 3 (46 mg, 0.104 mmol), 3-(R)-t-Boc-aminopyrrolidine (58 mg, 0.312 mmol), and pyridine (6 mL) was stirred under reflux for 36 h. TLC (DCM:MeOH = 40:1) showed the reaction was complete, and the solvent was removed using a rotary evaporator. The residue was purified by PTLC (DCM:MeOH = 40:1) to give 38 mg (60.3%) of product as a yellow powder: mp = 189–191 °C. <sup>1</sup>H NMR (CDCl<sub>3</sub>):  $\delta$  8.28 (m, 2H), 8.02 (d, 1H, *J* = 9.1 Hz), 7.75 (m, 1H), 7.65 (d, 1H, *J* = 9.1 Hz), 7.57 (m, 3H), 7.42 (d, 1H, *J* = 13.9 Hz), 4.28 (q, 2H, *J* = 7.1 Hz), 4.25 (m, 1H), 3.73 (m, 2H), 3.48 (m, 2H), 2.17 (m, 1H), 1.95 (m, 1H), 1.52 (s, 9H), 1.36 (t, 3H, *J* = 7.1 Hz). MS (CI) *m/z* 610 (MH<sup>+</sup>).

**Ethyl (S)-1-(3-(tert-Butoxycarbonylamino)pyrrolidin-1-yl)-2-fluoro-4-oxo-4H-pyrido[3,2,1-kl]naphtho[2,1-f]phenoxazine-5-carboxylate (6).** Following the procedure for compound 4 but with 3-(S)-t-Boc-aminopyrrolidine in place of 3-(R)-t-Boc-aminopyrrolidine, the titled product was obtained (36 mg, 57.1%) as a yellow powder: mp = 189–191 °C. <sup>1</sup>H NMR (CDCl<sub>3</sub>):  $\delta$  8.28 (m, 2H), 8.02 (d, 1H, *J* = 9.1 Hz), 7.75 (m, 1H), 7.65 (d, 1H, *J* = 9.1 Hz), 7.57 (m, 3H), 7.42 (d, 1H, *J* = 13.9 Hz), 4.28 (q, 2H, *J* = 7.1 Hz), 4.25 (m, 1H), 3.73 (m, 2H), 3.48 (m, 2H), 2.17 (m, 1H), 1.95 (m, 1H), 1.52 (s, 9H), 1.36 (t, 3H, *J* = 7.1 Hz). MS (CI) *m/z* 610 (MH<sup>+</sup>).

**(S)-1-(3-Aminopyrrolidin-1-yl)-2-fluoro-4-oxo-4H-pyrido[3,2,1-kl]naphtho[2,1-f]phenoxazine-5-carboxylic Acid Hydrogen Chloride Salt (7 or CS).** A mixture of compound 6 (36 mg, 0.06 mmol), KOH (17 mg, 0.30 mmol), ethanol (2 mL), and water (1 mL) was refluxed for 1 h. After cooling, 20% HCl (1 mL) was added, and the mixture was refluxed for 5 h. The precipitate was collected, washed with water, and dried over a vacuum pump to give 24 mg (78.3%) of CS as a yellow powder: mp = 260 °C (dec). <sup>1</sup>H NMR (DMSO-*d*<sub>6</sub>):  $\delta$  9.17 (s,

1H), 8.77 (s, 1H), 8.64 (d, 1H,  $J = 8.5$  Hz), 8.22 (d, 1H,  $J = 8.5$  Hz), 8.04 (m, 3H), 7.70 (m, 2H), 7.44 (d, 1H,  $J = 13.7$  Hz), 3.87 (m, 5H), 2.41 (m, 1H), 2.16 (m, 1H). MS (CI)  $m/z$  482 (MH<sup>+</sup>). Anal: (C<sub>28</sub>H<sub>21</sub>ClFN<sub>3</sub>O<sub>4</sub>, 0.5 H<sub>2</sub>O) C, H, N.

**(R)-1-(3-Aminopyrrolidin-1-yl)-2-fluoro-4-oxo-4H-pyrido[3,2,1-k]naphtho[2,1-f]phenoxazine-5-carboxylic Acid Hydrogen Chloride Salt (5 or CR).** Following the same procedure for compound 7, but with compound 4 (38 mg, 0.062 mmol) in place of 6, the titled product was obtained (27 mg, 84.4%) as a yellow powder: mp = 260 °C (dec). <sup>1</sup>H NMR (DMSO-*d*<sub>6</sub>): δ 9.17 (s, 1H), 8.77 (s, 1H), 8.64 (d, 1H,  $J = 8.5$  Hz), 8.22 (d, 1H,  $J = 8.5$  Hz), 8.04 (m, 3H), 7.70 (m, 2H), 7.44 (d, 1H,  $J = 13.7$  Hz), 3.87 (m, 5H), 2.41 (m, 1H), 2.16 (m, 1H). MS (CI)  $m/z$  482 (MH<sup>+</sup>). Anal: (C<sub>28</sub>H<sub>21</sub>ClFN<sub>3</sub>O<sub>4</sub>, 0.25 H<sub>2</sub>O) C, H, N.

**Ethyl 3-(3-Hydroxyphenanthren-2-ylamino)-2-(2,3,4,5-tetrafluorobenzoyl)acrylate (8).** Following the procedure for compound 2, but with 2-amino-3-hydroxyphenanthrene hydrochloride (170 mg, 0.58 mmol) in place of 2-amino-1-hydroxyphenanthrene hydrochloride, the titled product was obtained (231 mg, 69.2%) as a yellow powder: <sup>1</sup>H NMR (DMSO-*d*<sub>6</sub>): δ 8.93 (d, 1H,  $J = 14.3$  Hz), 8.83 (m, 1H), 8.46 (d, 1H,  $J = 14.3$  Hz), 8.30 (s, 1H), 8.19 (s, 1H), 7.92 (m, 1H), 7.81 (m, 1H), 7.60–7.50 (m, 3), 4.07 (q, 2H,  $J = 7.1$  Hz), 1.09 (t, 3H,  $J = 7.1$  Hz). MS (CI)  $m/z$  484 (MH<sup>+</sup>).

**Ethyl 1,2-Difluoro-4-oxo-4H-pyrido[3,2,1-k]naphtho[1,2-g]phenoxazine-5-carboxylate (9).** Following the procedure for compound 3, but with compound 8 (196 mg, 0.4 mmol) in place of 2, the titled product was obtained (149 mg, 82.9%) as a gray powder: mp = 235–237 °C. <sup>1</sup>H NMR (DMSO-*d*<sub>6</sub>): δ 9.03 (s, 1H), 8.64 (m, 1H), 8.40 (s, 1H), 8.34 (s, 1H), 7.74 (m, 1H), 7.71 (s, 1H), 7.63 (d, 1H,  $J = 9.6$  Hz), 7.51 (m, 2H), 7.43 (d, 1H,  $J = 9.6$  Hz), 4.33 (q, 2H,  $J = 7.1$  Hz), 1.37 (t, 3H,  $J = 7.1$  Hz). MS (CI)  $m/z$  444 (MH<sup>+</sup>).

**Ethyl (R)-1-(3-(tert-Butoxycarbonylamino)pyrrolidin-1-yl)-2-fluoro-4-oxo-4H-pyrido[3,2,1-k]naphtho[1,2-g]phenoxazine-5-carboxylate (10).** Following the procedure for compound 4, but with compound 9 (50 mg, 0.11 mmol) in place of 3, the titled product was obtained (54 mg, 78.3%) as a yellow powder: mp = 231–233 °C. <sup>1</sup>H NMR (CDCl<sub>3</sub>): δ 8.79 (s, 1H), 8.43 (d, 1H,  $J = 7.5$  Hz), 8.03 (s, 1H), 7.76 (d, 1H,  $J = 7.5$  Hz), 7.62–7.45 (m, 6H), 4.40 (q, 2H,  $J = 7.3$  Hz), 4.01–3.84 (m, 2H), 3.60–3.52 (m, 2H), 2.27–2.20 (m, 1H), 2.17–1.96 (m, 1H), 1.49 (s, 9H), 1.43 (t, 3H,  $J = 7.3$  Hz). MS (CI)  $m/z$  610 (MH<sup>+</sup>).

**Ethyl (S)-1-(3-(tert-Butoxycarbonylamino)pyrrolidin-1-yl)-2-fluoro-4-oxo-4H-pyrido[3,2,1-k]naphtho[1,2-g]phenoxazine-5-carboxylate (12).** Following the procedure for compound 6, but with compound 9 (50 mg, 0.11 mmol) in place of 3, the titled product was obtained (62 mg, 89.9%) as a yellow powder: mp = 231–233 °C. <sup>1</sup>H NMR (CDCl<sub>3</sub>): δ 8.79 (s, 1H), 8.43 (d, 1H,  $J = 7.5$  Hz), 8.03 (s, 1H), 7.76 (d, 1H,  $J = 7.5$  Hz), 7.62–7.45 (m, 6H), 4.40 (q, 2H,  $J = 7.3$  Hz), 4.01–3.84 (m, 2H), 3.60–3.52 (m, 2H), 2.27–2.20 (m, 1H), 2.17–1.96 (m, 1H), 1.49 (s, 9H), 1.43 (t, 3H,  $J = 7.3$  Hz). MS (CI)  $m/z$  610 (MH<sup>+</sup>).

**(S)-1-(3-Aminopyrrolidin-1-yl)-2-fluoro-4-oxo-4H-pyrido[3,2,1-k]naphtho[1,2-g]phenoxazine-5-carboxylic Acid Hydrogen Chloride Salt (13).** Following the same procedure for compound 7, but with compound 12 (50 mg, 0.082 mmol) in place of 6, the titled product was obtained (35 mg, 85%) as a yellow powder: mp = 246 °C (dec). <sup>1</sup>H NMR (DMSO-*d*<sub>6</sub>): δ 9.25 (s, 1H), 8.17 (d, 1H,  $J = 13.6$ ), 8.58 (s, 1H), 8.53 (s, 1H), 7.86 (m, 1H), 7.82 (s, 1H), 7.68 (d, 1H,  $J = 9.0$  Hz), 7.61 (m, 2H), 7.40 (d, 1H,  $J = 13.6$  Hz), 4.09 (m, 1H), 4.94 (m, 4H), 2.35 (m, 1H), 2.14 (m, 1H). MS (CI)  $m/z$  482 (MH<sup>+</sup>). Anal: (C<sub>28</sub>H<sub>21</sub>ClFN<sub>3</sub>O<sub>4</sub>, 0.75 H<sub>2</sub>O) C, H, N.

**(R)-1-(3-Aminopyrrolidin-1-yl)-2-fluoro-4-oxo-4H-pyrido[3,2,1-k]naphtho[1,2-g]phenoxazine-5-carboxylic Acid Hydrogen Chloride Salt (11).** Following the same procedure for compound 7, but with compound 10 (50 mg, 0.082 mmol) in place of 6, the titled product was obtained (34 mg, 80%) as a yellow powder: mp = 246 °C (dec). <sup>1</sup>H NMR (DMSO-*d*<sub>6</sub>): δ 9.25 (s, 1H), 8.17 (d, 1H,  $J = 13.6$ ), 8.58 (s, 1H), 8.53 (s, 1H), 7.86 (m, 1H), 7.82 (s, 1H), 7.68 (d, 1H,  $J = 9.0$  Hz), 7.61 (m, 2H), 7.40 (d, 1H,  $J = 13.6$  Hz), 4.09 (m, 1H), 4.94 (m, 4H),

2.35 (m, 1H), 2.14 (m, 1H). MS (CI)  $m/z$  482 (MH<sup>+</sup>). Anal: (C<sub>28</sub>H<sub>21</sub>ClFN<sub>3</sub>O<sub>4</sub>, 0.5 H<sub>2</sub>O) C, H, N.

**Materials for Biochemistry.** Compound solutions were prepared as 1 mM stock solutions in dimethyl sulfoxide and stored at –20 °C. These stock solutions were diluted to working concentrations in distilled water immediately before use. Electrophoretic reagents (acrylamide/bisacrylamide solution and ammonium persulfate) were purchased from BioRad, and *N,N,N',N'*-tetramethylethylenediamine (TEMED) was purchased from Fisher. T4 polynucleotide kinase, *Taq* DNA polymerase, and human topoisomerase II were purchased from New England Biolabs, Promega, and TopoGen, respectively. [ $\gamma$ -<sup>32</sup>P] ATP was purchased from NEN Dupont.

**Preparation and End-Labeling of Oligonucleotides.** Oligonucleotides were synthesized on an Expedite 8909 nucleic acid synthesis system (PerSeptive Biosystems, Framingham, MA) using the phosphoramidite method. The oligonucleotides were eluted out of the column by using aqueous ammonia and deprotected by heating at 55 °C overnight, followed by 15% denaturing polyacrylamide gel purification. Prior to the experiment, all oligonucleotides were treated in 10 mM NaOH for 30 min at 37 °C followed by neutralization with 10 mM HCl and ethanol precipitation in order to disrupt the self-associated structures. The 5'-end-labeled single-strand oligonucleotide was obtained by incubating the oligomer with T4 polynucleotide kinase and [ $\gamma$ -<sup>32</sup>P]ATP for 1 h at 37 °C. Labeled DNA was purified with a Bio-Spin 6 chromatography column (BioRad) after inactivating the kinase by heating for 8 min at 70 °C.

**Polymerase Stop Assay.** The DNA primer d[TAATAC-GACTCACTATAG] and template DNA HT4, d[TCCAACATG-TGTATAC(TTAGGG)<sub>4</sub>TTAGCGGCACGCAATTGCTATAGT-GAGTCGTATTA], or PQ74, d[TCCAACATGCTATAC(TTGGGG)<sub>4</sub>-TTAGCGGCACGCAATTGCTATAGTGAGCGTATTA], were synthesized and purified as mentioned above. Labeled primer (15 nM) and template DNA (10 nM) were annealed in a reaction buffer (50 mM Tris-HCl, pH 7.5, 10 mM MgCl<sub>2</sub>, 0.5 mM DTT, 0.1 mM EDTA, and 1.5 μg/μL BSA) with 0.1 mM dNTP by heating to 95 °C and then slowly cooled to room temperature.<sup>22</sup> KCl and NaCl (60 mM each) were added to the reaction with DNA containing a human telomeric sequence, and 5 mM of each salt was added to the reaction with DNA containing a *Tetrahymena* telomeric sequence. *Taq* DNA polymerase was added, and the mixture was incubated at 55 °C for 20 min. The polymerase extension was stopped by adding 2× stop buffer (10 mM EDTA, 10 mM NaOH, 0.1% xylene cyanole, 0.1% bromophenol blue in formamide solution) and loaded onto a 12% denaturing gel.

**Methylation Protection.** A methylation protection experiment was performed after the incubation of oligonucleotides with compounds, as described above. For each reaction, 10 μL of sample was mixed with 200 μL of reaction buffer (50 mM sodium cacodylate, pH 8.0, 1 mM EDTA) and 1 μL of 100% dimethyl sulfate (DMS). The reaction was stopped with 50 μL of DMS stop buffer (1.5 M sodium acetate, pH 7.0, 1 M β-mercaptoethanol, 100 μg/mL calf thymus DNA). DNA samples were then subjected to ethanol precipitation, piperidine treatment, and 12% denaturing polyacrylamide gel electrophoresis.

**Photomediated Strand Cleavage Reaction.** Labeled template PQ74 (10 nM) was heated to 95 °C and slowly cooled to room temperature in a buffer (50 mM Tris-HCl, pH 7.5, 5 mM NaCl, 5 mM KCl, 10 mM MgCl<sub>2</sub>, 0.5 mM DTT, 0.1 mM EDTA, and 1.5 μg/μL BSA). A 1 mM final concentration of FQA was added and transferred to a 24-well Titertek microtiter plate (ICN). This plate was placed on top of a Pyrex glass shield and irradiated for 2 h with an 85-W xenon lamp placed under the Pyrex glass. Pyrex glass was used to filter the UV light under 300 nm, thereby eliminating DNA damage caused directly by UV irradiation. During the irradiation, the Titertek plate was rotated three times to eliminate light heterogeneity. Reactions were terminated by the addition of 10 μg of calf thymus DNA, followed by phenol–chloroform extraction and ethanol precipitation. The resulting samples were subjected



to treatment with 0.1 M piperidine. The samples were then loaded onto a 12% sequencing gel.

**kDNA Decatenation Assay.** kDNA (0.25  $\mu$ g) was incubated with various concentrations of FQA or A-62176 in 10  $\mu$ L of reaction buffer (50 mM Tris-HCl, pH 8.0, 120 mM KCl, 10 mM MgCl<sub>2</sub>, 0.5 mM ATP, and 0.5 mM dithiothreitol) for 10 min. Two units of human topoisomerase II were added to the mixture, which was then incubated at 37 °C for 30 min. The reaction was terminated with 0.1 volume of stop buffer (5% sarkosyl, 0.025% bromophenol blue, 50% glycerol). The decatenation products were analyzed on 1% agarose gels and run with 0.5  $\mu$ g/mL ethidium bromide.

**Topoisomerase II Cleavage Reaction.** Oligomers A1, d[CGATGGGGAAGATCGGGCTCGTATACATTGATACGGG-GCTCATGAGCGCTTGTTCGGCG], and A2, d[CGCCGAA-ACAAGCGCTCATGAGCCCCGTATCAATGTATACGAGCCCGATCTTCCCCATCG], were synthesized as mentioned above. The 5'-end-labeled A1 was annealed with the complementary strand (A2) by heating to 95 °C and slowly cooled to room temperature. Labeled double-stranded DNA was purified on an 8% native polyacrylamide gel. DNA was incubated with 20 units of human topoisomerase II in 20  $\mu$ L of reaction buffer (30 mM Tris-HCl, pH 7.6, 3 mM ATP, 15 mM  $\beta$ -mercaptoethanol, 8 mM MgCl<sub>2</sub>, 60 mM NaCl) at 30 °C for 10 min in the presence of various concentrations of compounds. Reactions were terminated by adding SDS to 1% of the final concentration, and topoisomerase II was removed by proteinase K digestion (100  $\mu$ g/mL) at 42 °C for 1 h followed by phenol/chloroform extraction and ethanol precipitation. Samples were loaded onto a 12% denaturing sequencing gel.

**Imaging and Quantification.** The dried gels were exposed on a phosphor screen. Imaging and quantification were performed using a PhosphorImager (Storm 820) and ImageQuant 5.1 software from Molecular Dynamics.

**Cytotoxicity Assay.** MCF7 human breast cancer cells were purchased from the American Tissue Culture Collection (Rockville, MD) and cultured according to the supplier's instructions. 8226/S and 8226/DOX1V were kindly provided by Dr. William S. Dalton (College of Medicine, The University of Arizona) and cultured according to the literature.<sup>27</sup> Exponentially growing cells (1–2  $\times$  10<sup>3</sup> cells) in 0.1 mL of medium were seeded on day 0 in a 96-well microtiter plate. On day 1, 0.1 mL aliquots of medium containing graded concentrations of compound were added to the cell plates. On day 4, the cell cultures were incubated with 50  $\mu$ L of 3-(4,5-dimethylthiazol-2-yl)-2,5-diphenyltetrazolium bromide (1 mg/mL in Dulbecco's phosphate buffered saline) for 4 h at 37 °C. The resulting formazan precipitate was solubilized with 200  $\mu$ L of 0.04 M HCl in isopropyl alcohol. For determination of the IC<sub>50</sub> values, the absorbance readings at 570 nm were fitted to the four-parameter logistic equation.

SW39 [telomerase (+)/ALT (-)] and SW26 [telomerase (-)/ALT (+)] were generously supplied by Dr. Jerry W. Shay (University of Texas, Southwestern Medical Center). Briefly, IMR90 cells were immortalized by SV40 T-antigen oncoprotein and separated into two subtypes: telomerase (+)/ALT (-) (SW39) and telomerase (-)/ALT (+) (SW26). Cultures were maintained at 37 °C, 5% CO<sub>2</sub> in a 4:1 mixture of Dulbecco's MEM and medium 199 (CellGro) supplemented with 10% fetal bovine serum and 100 units/mL penicillin/streptomycin (Omega Scientific). SW26 and SW39 cells were seeded at 0.4 and 0.2 million cells per 75 cm<sup>2</sup> flask, respectively. Cells were passaged every 6–7 days, counted by hemocytometer, and reseeded at the original concentration.

**Acknowledgment.** This research was supported by the National Institutes of Health (CA88310 and CA94166). We are grateful to Dr. William S. Dalton (The University of Arizona) and Dr. Jerry W. Shay (University of Texas, Southwestern Medical Center) for providing the cell lines and to Dr. Elzbieta Izbicka (Institute for Drug Development, San Antonio, TX) and Dr. David Nishioka (Georgetown University) for the sea urchin

embryo experiments. We thank Dr. Evonne Rezler for critical reading of drafts of the manuscript and Dr. David Bishop for preparing, proofreading, and editing the final version of the manuscript and figures.

## References

- Wang, J. C. DNA topoisomerases. *Annu. Rev. Biochem.* **1996**, *6*, 635–692.
- Reece, R. J.; Maxwell, A. DNA gyrase: structure and function. *CRC Crit. Rev. Biochem. Mol. Biol.* **1991**, *26*, 335–375.
- Nitiss, J. L. Investigating the biological functions of DNA topoisomerases in eukaryotic cells. *Biochim. Biophys. Acta* **1998**, *1400*, 63–81.
- Wang, J. C. Cellular roles of DNA topoisomerases: a molecular perspective. *Nat. Rev. Mol. Cell Biol.* **2002**, *3*, 430–440.
- Liu, L. F. DNA topoisomerase poisons as antitumor drugs. *Annu. Rev. Biochem.* **1989**, *58*, 351–375.
- Pommier, Y. In *Cancer Therapeutics: Experimental and Clinical Agents*; Teicher, B. A., Ed.; Humana Press: Totowa, NJ, 1997; pp 153–174.
- Chen, A. Y.; Liu, L. F. DNA topoisomerases—essential enzymes and lethal targets. *Annu. Rev. Pharmacol. Toxicol.* **1994**, *34*, 191–218.
- Chu, D. T. W.; Maleczka, R. E. J. Synthesis of 4-oxo-4H-quinolo[2,3,4-i,j][1,4]benoxazine-5-carboxylic acid derivatives. *J. Heterocycl. Chem.* **1987**, *24*, 453–456.
- Chu, D. T. W.; Hallas, R.; Clement, J. J.; Alder, L.; McDonald, E.; Plattner, J. J. Synthesis and antitumor activities of quinolone antineoplastic agents. *Drug Exp. Clin. Res.* **1992**, *18*, 275–282.
- Clement, J. J.; Burres, N.; Jarvis, K.; Chu, D. T. W.; Swinarski, J.; Adler, J. Biological characterization of a novel antitumor quinolone. *Cancer Res.* **1995**, *55*, 830–835.
- Permana, P. A.; Snapka, R. M.; Shen, L. L.; Chu, D. T. W.; Clement, J. J.; Plattner, J. J. Quinobenzoxazines: a class of novel antitumor quinolones and potent mammalian DNA topoisomerase II catalytic inhibitors. *Biochemistry* **1994**, *33*, 11333–11339.
- Kwok, Y.; Zeng, Q.; Hurley, L. H. Structural insight into a quinolone-topoisomerase II-DNA complex. Further evidence for a 2:2 quinobenzoxazine-Mg<sup>2+</sup> self-assembly model formed in the presence of topoisomerase II. *J. Biol. Chem.* **1999**, *274*, 17226–17235.
- Duan, W.; Vankayalapati, H.; Rangan, A.; Kim, M.-Y.; Sun, D.; Han, H.; Izbicka, E.; Nishioka, D.; Rha, S. Y.; Von Hoff, D. D.; Hurley, L. H. Design and synthesis of fluoroquinophenoxazines that interact with G-quadruplexes and their biological effects. *Mol. Cancer Ther.* **2001**, *1*, 103–120.
- Zahler, A. M.; Williamson, J. R.; Cech, T. R.; Prescott, D. M. Inhibition of telomerase by G-quartet DNA structures. *Nature* **1991**, *350*, 718–720.
- Sun, D.; Thompson, B.; Cathers, B. E.; Salazar, M.; Kerwin, S. M.; Trent, J. O.; Jenkins, T. C.; Neidle, S.; Hurley, L. H. Inhibition of human telomerase by a G-quadruplex-interactive compound. *J. Med. Chem.* **1997**, *40*, 2113–2116.
- Neidle, S.; Parkinson, G. Telomere maintenance as a target for anticancer drug discovery. *Nature Rev. Drug Discovery* **2002**, *1*, 383–393.
- Riou, J. F.; Guittat, L.; Mailliet, P.; Laoui, A.; Renou, E.; Petitgenet, O.; Megnin-Chanet, F.; Hélène, C.; Mergny, J. L. Cell senescence and telomere shortening induced by a new series of specific G-quadruplex DNA ligands. *Proc. Natl. Acad. Sci. U.S.A.* **2002**, *5*, 2672–2677.
- Gowan, S. M.; Heald, R.; Stevens, M. F.; Kelland, L. R. Potent inhibition of telomerase by small-molecule pentacyclic acridines capable of interacting with G-quadruplexes. *Mol. Pharmacol.* **2001**, *60*, 981–988.
- Gowan, S. M.; Harrison, J. R.; Patterson, L.; Valenti, M.; Read, M. A.; Neidle, S.; Kelland, L. R. A G-quadruplex-interactive potent small-molecule inhibitor of telomerase exhibiting *in vitro* and *in vivo* antitumor activity. *Mol. Pharmacol.* **2002**, *61*, 1154–1162.
- Grand, C. L.; Han, H.; Muñoz, R. M.; Weitman, S.; Von Hoff, D. D.; Hurley, L. H.; Bearss, D. J. The cationic porphyrin TMPyP4 downregulates c-MYC and hTERT expression and inhibits tumor growth *in vivo*. *Mol. Cancer Ther.* **2002**, *1*, 565–573.
- Zeng, Q.; Kwok, Y.; Kerwin, S. M.; Mangold, G.; Hurley, L. H. Design of new topoisomerase II inhibitors based upon a quinobenzoxazine self-assembly model. *J. Med. Chem.* **1998**, *41*, 4273–4278.
- Han, H.; Hurley, L. H.; Salazar, M. A DNA polymerase stop assay for G-quadruplex-interactive compounds. *Nucleic Acids Res.* **1999**, *27*, 537–542.
- Weitzmann, M. N.; Woodford, K. J.; Usdin, K. The development and use of a DNA polymerase arrest assay for the evaluation of parameters affecting intrastrand tetraplex formation. *J. Biol. Chem.* **1996**, *271*, 20958–20964.



- (24) Maxam, A.; Gilbert, W. Sequencing end-labeled DNA with base-specific chemical cleavages. *Methods Enzymol.* **1980**, *65*, 499–560.
- (25) Arimondo, P. B.; Riou, J. F.; Mergny, J. L.; Tazi, J.; Sun, J. S.; Garestier, T.; Hélène, C. Interaction of human DNA topoisomerase I with G-quartet structures. *Nucleic Acids Res.* **2000**, *28*, 4832–4838.
- (26) Marini, J. C.; Miller, K. G.; Englund, P. T. Decatenation of kinetoplast DNA by topoisomerase. *J. Biol. Chem.* **1980**, *255*, 4976–4979.
- (27) Wang, H.; Jiang, Z.; Wong, Y. W.; Dalton, W. S.; Futscher, B. W.; Chan, V. T. Decreased CP-1 (NF-Y) activity results in transcriptional down-regulation of topoisomerase II $\alpha$  in a doxorubicin-resistant variant of human multiple myeloma RPMI 8226. *Biochem. Biophys. Res. Commun.* **1997**, *237*, 217–224.
- (28) Holt, S. E.; Glinsky, V. V.; Ivanova, A. B.; Glinsky, G. V. Resistance to apoptosis in human cells conferred by telomerase function and telomere stability. *Mol. Carcinogenesis* **1999**, *25*, 241–248.
- (29) Dunham, M. A.; Neumann, A. A.; Fasching, C. L.; Reddel, R. R. Telomere maintenance by recombination in human cells. *Nat. Genet.* **2000**, *26*, 447–450.
- (30) Yu, H.; Hurley, L. H.; Kerwin, S. M. Evidence for the formation of 2:2 drug–Mg<sup>2+</sup> dimers in solution and for the formation of dimeric drug complexes on DNA from the DNA-accelerated photochemical reaction of antineoplastic quinobenzoxazines. *J. Am. Chem. Soc.* **1996**, *118*, 7040–7048.
- (31) Chong, L.; van Steensel, B.; Broccoli, D.; Erdjument-Bromage, H.; Hanish, J.; Tempst, P.; de Lange, T. A human telomeric protein. *Science* **1995**, *270*, 1663–1667.
- (32) Billaud, T.; Brun, C.; Ancelin, K.; Koering, C. E.; Laroche, T.; Gilson, E. Telomeric localization of TRF2, a novel human telobox protein. *Nat. Genet.* **1997**, *17*, 236–239.
- (33) Broccoli, D.; Godley, L. A.; Donehower, L. A.; Varmus, H. E.; de Lange, T. Telomerase activation in mouse mammary tumors: lack of telomere shortening and evidence for regulation of telomerase RNA with cell proliferation. *Mol. Cell. Biol.* **1996**, *16*, 3765–3772.
- (34) Griffith, J. D.; Comeau, L.; Rosenfield, S.; Stansel, R. M.; Bianchi, A.; Moss, H.; de Lange, T. Mammalian telomeres end in a large duplex loop. *Cell* **1999**, *97*, 503–514.
- (35) Karlseder, J.; Smogorzewska, A.; de Lange, T. Senescence induced by altered telomere state, not telomere loss. *Science* **2002**, *295*, 2446–2449.
- (36) Han, H.; Bennett, R. J.; Hurley, L. H. Inhibition of unwinding of G-quadruplex structures by Sgs1 helicase in the presence of *N, N*-bis[2-(1-piperidino)ethyl]-3,4,9,10-perylenetetracarboxylic diimide, a G-quadruplex-interactive ligand. *Biochemistry* **2000**, *39*, 9311–9316.
- (37) Parkinson, G. N.; Lee, M. P. H.; Neidle, S. Crystal structure of parallel quadruplexes from human telomeric DNA. *Nature* **2002**, *417*, 876–880.
- (38) Wang, Y.; Patel, D. J. Solution structure of the human telomeric repeat d[AG<sub>3</sub>(T<sub>2</sub>AG<sub>3</sub>)<sub>3</sub>] G-tetraplex. *Structure* **1993**, *1*, 263–282.
- (39) Calder, I. C.; Williams, P. J. The synthesis and reactions of some carcinogenic *N*-(2-phenanthryl)hydroxylamine derivatives. *Aust. J. Chem.* **1974**, *27*, 1791–1795.

JM0203377